Image Deconvolution Using Incomplete Fourier Measurements

Hang Yang,[1] Zhongbo Zhang,[2] Danyang Wu[2]

[1] Changchun Institute of Optics, Fine Mechanics and Physics, Chinese Academy of Science, Changchun 130033, PR China

[2] School of Mathematics, Jilin University, Changchun 130012, PR China

Received 5 December 2011; accepted 10 September 2012

ABSTRACT: In this article, we propose a new deconvolution algorithm, which is based on image reconstruction from incomplete measurements in Fourier domain. Our algorithm has two steps. First, an initial estimator is obtained using Fourier regularized inverse operator. Second, parts of the estimator's Fourier coefficients are saved, and the others are removed to suppress noise energy, then the remaining coefficients are used to recover image based on the sparse constraints. This image reconstruction problem is an optimization problem that is solved by a fast algorithm named split Bregman iteration. Different from other deconvolution algorithms, our algorithm only uses parts of Fourier components to restore the blurred image and combines two different regularization strategies efficiently by applying a selection matrix. The experiment shows that our method gives better performance than many other competitive deconvolution methods. © 2012 Wiley Periodicals, Inc. Int J Imaging Syst Technol, 22, 233–240, 2012; Published online in Wiley Online Library (wileyonlinelibrary.com). DOI 10.1002/ima.22027

Key words: image deconvolution; image deblurring; split Bregman iteration; incomplete measurements

I. INTRODUCTION

Image deconvolution is an inverse problem existing in a wide variety of image processing fields, including physical, optical, medical, and astronomical applications. For example, practical satellite images are often blurred because of the limitations such as aperture effects of the camera, camera motion, and atmospheric turbulence (Jain, 1989). Deconvolution becomes necessary when we wish a crisp deblurred image for viewing or further processing.

A digitally recorded image is a finite discrete data set, so the image deconvolution problem is formulated as a matrix inversion problem. The observed samples y consist of unknown desired signal samples x first degraded by convolution (denoted by ''$\circledast$'') with a known impulse response h from a linear time-invariant system H and then corrupted by zero mean additive white Gaussian noise (AWGN) γ with variance σ^2. The formulation of blurring often can be described as

$$y(n) = Hx(n) + \gamma(n) = (h \circledast x)(n) + \gamma(n). \tag{1}$$

Equation (1) in the discrete Fourier transform (DFT) domain can be written as

$$Y(k) = H(k)X(k) + \Gamma(k), \tag{2}$$

where $Y(k)$, $H(k)$, $X(k)$ and $\Gamma(k)$ are the 2D DFTs of $y(n)$, $h(n)$, $x(n)$, and $\gamma(n)$, respectively. The goal of image deblurring is to recover clear image x from the blurred image y.

A naive deblurring estimate $\widetilde{x}$ is

$$\widetilde{x} = H^{-1}y = x + H^{-1}\gamma. \tag{3}$$

The deblurring process is a mathematically ill-posed problem, which can be interpreted as an inverting low-pass filtering, backward diffusion, or entropy decreasing. The variance of the colored noise $H^{-1}\gamma$ is large. In this case, the mean squared error between x and $\widetilde{x}$ is large, making $\widetilde{x}$ an unsatisfactory deconvolution estimate.

In recent years, lots of deconvolution algorithms have been proposed. Among these methods, the Wiener filter and the Tikhonov regularized can solve this problem in the frequency domain in a fast speed. However, they often obtain a noisy result with ringing effects. Increased performance of deconvolution methods can be attributed to the inclusion of the wavelet-based estimators. One such kind of technique called the wavelet–vaguelette deconvolution was proposed in Donoho (1995). In this work, functionals called vaguelettes are used to simultaneously deconvolve and compute the wavelet coefficients. However, the algorithm cannot provide good estimates for all convolution operators. To overcome this limitation, Kalifa et al. (2003) proposed a wavelet packet based method that matches the frequency behavior of certain convolution operators. More wavelet-based techniques have been proposed in Johnstone et al. (2004), Fan and Koo (2002), and Figueiredo and Nowak (2003).

In Neelamani et al. (2004), the authors proposed an improved hybrid Fourier-wavelet regularized deconvolution (ForWaRD)

Correspondence to: Hang Yang; e-mail: yanghang09@mails.jlu.edu.cn

algorithm with any ill-conditioned convolution system. This method uses Fourier-domain regularized inversion followed by wavelet-domain noise shrinkage to minimize the distortion of spatially localized features in the image. Two extensions in terms of curvelets and shearlets, known as ForCuRD and ShearDec, was proposed in Neelamani et al. (2007) and Patel et al. (2009), respectively. Additional, the local polynomial approximation (LPA-ICI; Katkovnik et al., 2005) algorithm performs better than some of the best existing deblurring methods in terms of improvement in signal-to-noise-ratio (ISNR).

The iterative deblurring method is another important category. The well-known basic iterative methods are Landweber (1951), Richardson (1972), and Lucy et al. (1974). Many extensions and improvements over these methods have been made that include the use of wavelets or other sparse representations, such as curvelets. The fast total variation based deconvolution (FTvd; Wang et al., 2008) and TV based deconvolution using Bregman iteration (TV Bregman; Osher et al., 2005), which are well known of edge-preserving, can generally achieve good results. This total variation (TV) deconvolution method finds approximate solutions to differential equations in the space of bounded variation functions. Some of these are Starck et al. (2003), Elad et al. (2007), Takeda et al. (2008), Fadili and Starck (2007), Vonesch and Unser (2008), and Chang and Chen (2004). Note some of the these iterative techniques make use of L1-norm transform domain sparsity promotion.

In this article, we propose a new approach to solve the convolution problem based on image reconstruction from incomplete measurements in Fourier domain. Our approach has two steps. First, we obtain an initial estimator based on Fourier domain regularized inverse operator. Second, we select parts of the frequency domain information (the Fourier coefficients that keep the main energy of image but little noise energy), and then those measurements are used to reconstruct the whole image based on the sparse constraints, and the sparsity regularization terms enable the application of a new numerical algorithm, namely, split Bregman iteration, which can solve the proposed L1-norm minimization problem efficiently. Experimental results demonstrate the effectiveness of the proposed algorithm and show that it is better than many competitive deconvolution methods.

The remainder of this article is organized as follows. In Section II, we discuss the proposed deblurring algorithm in detail. In Section III, we show some simulation results and present the concluding remarks in Section IV.

II. DECONVOLUTION ALGORITHM

A. The Motivation. We established a method for obtaining an initial image estimate when the image is corrupted by colored noise, let us now focus on how we are to use this method as part of our deblurring routine. As blurring model is described by (1): $y = Hx + n = h \circledast x + \gamma$. A naive estimate is

$$\widetilde{x} = H^{-1}y = x + H^{-1}\gamma.$$

In the Fourier domain, the pseudoinversion operation of (1) can be rewritten as

$$\widetilde{X}(k) = \begin{cases} X(k) + \Gamma(k)/H(k), & \text{if} |H(k)| > 0, \\ 0, \text{otherwise}, \end{cases} \tag{4}$$

where $\widetilde{X}$ is the DFT of $\widetilde{x}$. Unfortunately, the variance of the colored noise $H^{-1}n$ in $\widetilde{x}$ is large, so $\widetilde{x}$ is an unsatisfactory deblurring estimate.

From (4), we can clearly see that the noise components where $|H(k)| \approx 0$ are particularly amplified. So if those components of the estimate $\widetilde{x}$ where $|H(k)| \approx 0$ are removed, can we use the remaining Fourier coefficients to reconstruct the original image? We consider to recover the image by solving an optimization problem based on the sparse constraints.

According to the fundamental principle of compressed sensing, the image can be recovered with incomplete measurements of it by optimization (Candes et al., 2006; Ma, 2011). The image can be reconstructed by solving:

$$\arg\min_u |\Phi u|_1 + \frac{\lambda}{2} \| g - Au \|_2^2, \tag{5}$$

where A is the measure matrix, Φ is a transform matrix, and $\lambda \geq 0$ is the regularization parameter.

Our problem is similar to (5), in which the L1-norm optimization problem is used to recover the clear image and obtain the estimate x^*:

$$x^* = \arg\min_u |\Phi u|_1 + \frac{\lambda}{2} \| g - R \cdot Fu \|_2^2, \tag{6}$$

where F is the Fourier transform matrix, R is a selection matrix, for example,

$$R(k) = \begin{cases} 1, & |H(k)| \geqslant \tau, \\ 0, & |H(k)| < \tau \end{cases} \tag{7}$$

and define $g = R \cdot F\widetilde{x}$.

Our method combines two different regularization procedures, Fourier regularization and iterative restoration procedure, determined by a selection matrix. The selection matrix is an important element for our algorithm, which is used to suppress the colored noise's energy and retain the main energy of image. Different from other deconvolution methods, we only use part of the information in the frequency domain to restore image, which could reduce the influence of noise and improve quality to image restoration.

Figure 1 illustrates a simple deconvolution result of our proposed method for the 2D $r = 4.5$ circular spot blur operator.

B. Improvement. Although we can obtain an estimate of the clear image from (6), the energy of noise is not suppressed in the remaining Fourier components. The Fourier domain provides the most economical representation of the colored noise $H^{-1}\gamma$, because the Fourier transform acts as the Karhunen–Loeve transform (Castleman, 1996) and decorrelates the noise $H^{-1}\gamma$. Consequently, among all linear transformations, the Fourier transform captures the maximum colored noise energy using a fixed number of coefficients (Davis, and Nosratinia, 1999). More details can be found in Neelamani et al. (2004) and Davis and Nosratinia (1999). So, we use Fourier shrinkage to attenuate the colored noise in $\widetilde{x}$.

An estimate of the power spectral density (PSD) can be accurately determined from a method such as that proposed in Hillery and Chin (1991), a Wiener-based solution can be found using

$$H_\alpha(k) = \frac{\overline{H}(k)}{|H(k)|^2 + \alpha \frac{M^2\sigma^2}{|P_{\text{sd}}(k)|^2}} \tag{8}$$

where σ^2 is the variance of noise, $\alpha \in R^+$, Psd is the estimated PSD of the image, and M is the size of image.

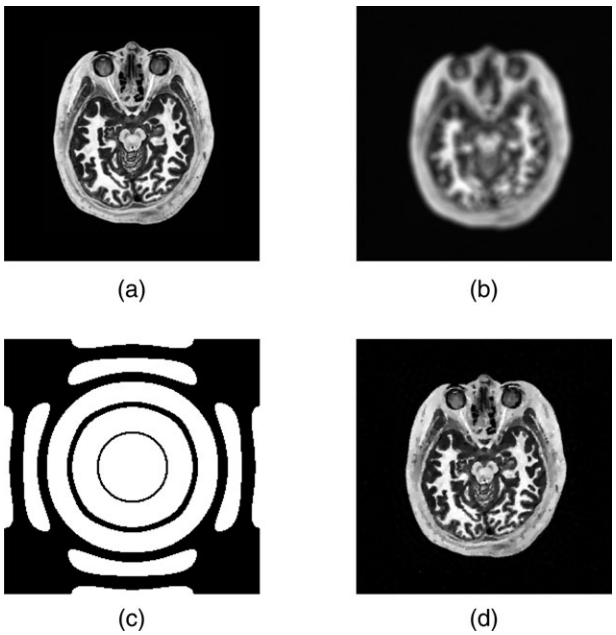

Figure 1. (a) Test medical image (256 × 256). (b) Observed image: smoothed by a 2-D $r = 4.5$ circular spot blur plus white Gaussian noise with variance such that the BSNR = 40 dB. (c) The selection matrix R, $\tau = 0.025$. (d) Our method estimate (ISNR = 9.46 dB).

Using the regularized inverse operator (8), we can obtain an initial estimate $\bar{x}_\alpha$, its Fourier transform $\overline{X}_\alpha$ is

$$\overline{X}_\alpha(k) = Y(k)H_\alpha(k) = X(k)\left(\frac{|H(k)|^2}{|H(k)|^2 + \alpha\frac{M^2\sigma^2}{|P_{sd}(k)|^2}}\right) + \frac{N(k)\overline{H}(k)}{|H(k)|^2 + \alpha\frac{M^2\sigma^2}{|P_{sd}(k)|^2}}, \quad (9)$$

From (9), both the noise energy and image energy in the estimate $\widetilde{X}_\alpha(k)$ are small in Fourier domain when $|H(k)|$ is small. So, they can hardly provide useful information for recovering. However, when $|H(k)|$ is large, the image energy is kept well and the energy of colored noise is suppressed.

We use the new estimate $\widetilde{x}_\alpha$ to replace $\widetilde{x}$ to reconstruct the image based on (6), but for this time, $g = R \cdot F\widetilde{x}_\alpha = R \cdot \widetilde{X}_\alpha$.

C. Minimization Based on Split Bregman Iterative. In this article, our approach to the solution of the L1-norm optimization problem (6) allows us to perform the minimization phase by some good method. We consider a fast iterative algorithm named split Bregman iteration, proposed in Goldstein and Osher (2009) for the image restoration problem.

Recently, split Bregman iteration attracts much attention in signal/image recovery. The basic idea is to transform a constrained optimization problem to a series of unconstrained problems. In each unconstrained problem, the object function is defined by Bregman distance (Bregman, 1967) of a convex functional. This is an extremely fast algorithm, very simple to program. So, it has been studied widely by researchers. The details of Bregman iteration will not be discussed here. Rather we refer the reader to Yin et al. (2008), Osher et al. (2005), and Cai et al. (2009, submitted for publication) An in-depth description of the application of this technique to the split Bregman method can be found in Goldstein and Osher (2009). Goldstein and Osher (2009) described its further applications in image processing, and the convergence analysis was given in Cai et al. (2009).

Split Bregman method has the advantage that it does not require regularization, continuation, or the enforcement of inequality constraints. Furthermore, the technique has been shown to be an extremely efficient solver for L1 regularized denoi!sing problems, as well as a large class of problems from compressed sensing.

Applying split Bregman iterative to problem (6), W being a transform matrix, we can have:

Split Bregman Iterative Algorithm for Recovering:

Initialize: $u^0 = F^{-1}g$, $d_x^0 = d_y^0 = b_x^0 = b_y^0$
while $\|R \cdot Fu - g\|_2^2 \geq \sigma^2$,do
  For k = 0,1,. . .,do
    $\text{rhs}^k = \mu F^T R \cdot g + \lambda\nabla_x^T(d_x^k - b_x) + \lambda\nabla_y^T(d_y^k - b_y) + \beta u$
    $u^{k+1} \leftarrow F^{-1}(F\text{rhs}^k./K)$
    $d_x^{k+1} \leftarrow \max(s^k - 1/\lambda, 0)\frac{\nabla_x u^k + b_x^k}{s^k}$
    $d_y^{k+1} \leftarrow \max(s^k - 1/\lambda, 0)\frac{\nabla_y u^k + b_y^k}{s^k}$
    $b_x^{k+1} \leftarrow b_x^k + \nabla_x u^{k+1} - d_x^{k+1}$
    $b_y^{k+1} \leftarrow b_y^k + \nabla_y u^{k+1} - d_y^{k+1}$
  end For
  $g^{k+1} \leftarrow g^k + g - R \cdot Fu^{k+1}$
end while

where $K = \mu R - \lambda F\Delta F^{-1} + \beta$, $s^k = \sqrt{|\nabla_x u^k + b_x^k|^2 + |\nabla_y u^k + b_y^k|^2}$ and ''shrink( )'' is the soft-threshold operator. When choosing $\Phi = \nabla$, let $\beta = 0$; while choosing Φ as a transform matrix, let $\lambda = 0$. There are more details in Goldstein and Osher (2009). This iterative may be a little different from the ''Constrained CS Optimization Algorithm'' in Goldstein and Osher (2009), but essentially the two algorithms are the same.

D. Summary and Implementation. From Sections II.B and II.C, we can see that our algorithm consists of the following three steps:

1. Select the Fourier coefficients that should be saved in Fourier domain, which is to determine the selection matrix R (7).
2. To suppress noise energy in the remaining Fourier components, use (9) to Y (the Fourier transform of the observed image y) to obtain $\widetilde{X}_\alpha$.
3. Apply split Bregman iterative to solve the sparse regularization (6), and obtain the estimate $\widehat{x}$.

Our method combines two different regularization procedures: In the second step, an efficient deconvolution method using fast Fourier transforms can be used; In the third step, effective methods like tight frame reconstruction method or TV reconstruction method can be used. We find that the components that are determined by the selection matrix R are useless for image deconvolution. So, we remove these image components and utilize the reminding components to reconstruct the whole image, which could reduce the noise influence and improve the restored image quality. The selection matrix R is an important element for our

Table 1. ISNR for different experiments

Methods	Our Method	LPA-ICI	For-WaRD	For-CuRD	FTVd	TV-Bregman
Exp. 1	8.14	7.84	7.40	7.28	7.10	7.83
Exp. 2	4.92	4.62	4.59	4.65	4.68	4.40
Exp. 3	1.42	1.00	1.12	1.03	1.10	0.95
Exp. 4	3.28	2.76	2.24	2.56	2.98	3.07
Exp. 5	5.54	4.85	4.73	4.53	4.77	5.16
Exp. 6	4.72	4.45	3.91	4.34	4.49	4.53
Exp. 7	5.53	5.08	4.54	4.27	4.95	5.28
Exp. 8	4.96	4.62	3.85	4.16	4.54	4.49
Exp. 9	5.65	4.17	3.91	4.53	–	–

algorithm, which suppresses the colored noise's energy and retains the main energy of image, and it is used to balance the influence of Fourier regularization and L1-norm optimization regularization. The parameter τ of R is a major parameter in this algorithm. It can affect the final result: the lower value may not suppress the colored noise influence enough, and a higher value may not keep the main energy of image well.

Different from other deconvolution methods, we only use part of the information in the frequency domain to restore image, which can reduce the influence of noise and improve quality of image restoration. The another advantage of this proposal is that the optimization problem in Step 2 permits fast and efficient algorithm and produce better restored images in visual quality and ISNR than those obtained using the combination of a data-fitting term and a regularization term together.

III. EXPERIMENTAL RESULTS

In this section, we present results of our proposed algorithm and compare them with some of the deconvolution methods such as ForWaRD (Neelamani et al., 2004), ForCuRD (Neelamani et al., 2007), LPA-ICI (Katkovnik et al., 2005), FTVd (Wang et al., 2008), and TVBregman (Osher et al., 2005). In these experiments, we will use the improvement in ISNR to measure the performance. The ISNR is defined as

$$\mathrm{ISNR} = 10\log_{10}\left(\frac{\| x-y \|_2^2}{\|x-\hat{x}\|_2^2}\right),$$

where y is the observed image, x is the original image, and $\hat{x}$ is the estimated image.

For an image of $M*M$ size, the blurred SNR(BSNR) is defined in decibels as

$$\mathrm{BSNR} = 10\log_{10}\left(\frac{\|x\circledast h - E(x\circledast h)\|_2^2}{M^2\sigma^2}\right),$$

where $E(x \circledast h)$ denotes the mean of $x \circledast h$.

In our experiments, we use anisotropic TV model for image recovering, that is to choose $\Phi = \nabla$. The anisotropic TV model can preserve the edge well. (We can also choose other transform matrices, such as wavelet and curvelet.) The parameter τ of R is hand tuned in each case for best ISNR, so that the comparison is carried out in the regime that is relevant in practice.

In the first set of tests, we consider the setup of Neelamani et al. (2004), where a Cameraman image is blurred by a 9×9 uniform box-car blur. The AWGN variance, σ^2 is chosen with a BSNR of 40 dB. A comparison of different methods in terms of ISNR is shown in Table I. Our proposed method yields a value 8.14 dB, which is better than the values obtained by any of the other methods, we can see that the selection matrix R is an important factor for improving restored quality. And our method is not slow, because the split Bregman iteration is a fast algorithm for image recovering. The images obtained by different methods are shown in Figure 2.

In the second set of tests, the original image of Lena is blurred by a Gaussian PSF defined as

$$h(i,j) = Ke^{-\frac{i^2+j^2}{2\eta^2}}$$

for $i,j = -5,..,5$, where K is a normalizing constant ensuring that the blur is of unit mass, and η^2 is the variance that determines the severity of the blur. In this experiment, we chose $\eta = 2$, the noise

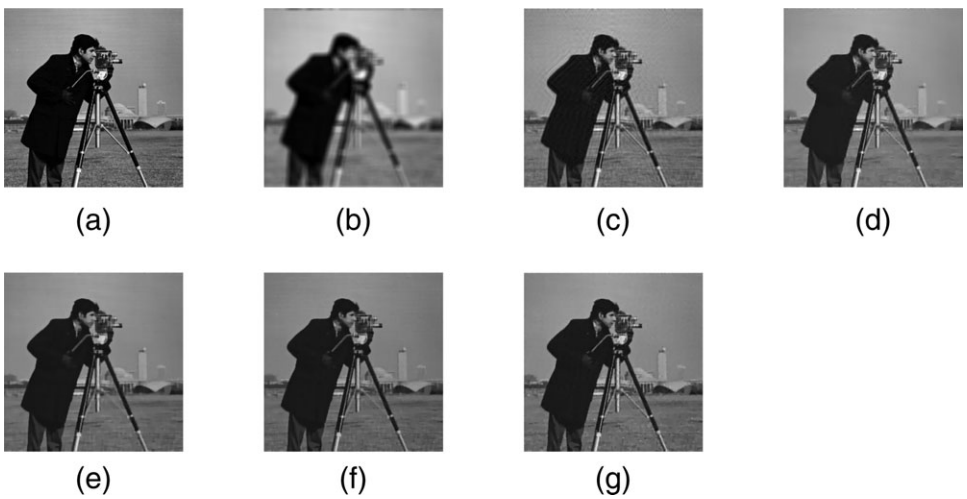

Figure 2. The results by different methods with a cameraman image. (a) Original image. (b) Noisy blurred image, BSNR = 40 dB. (c) ForCuRD estimate, ISNR = 7.28 dB. (d) ForWaRD estimate, ISNR = 7.40 dB. (e) FTVd estimate, ISNR = 7.10 dB. (f) TVBregman estimate, ISNR = 7.83 dB. (g) Our method estimate, ISNR = 8.14 dB.

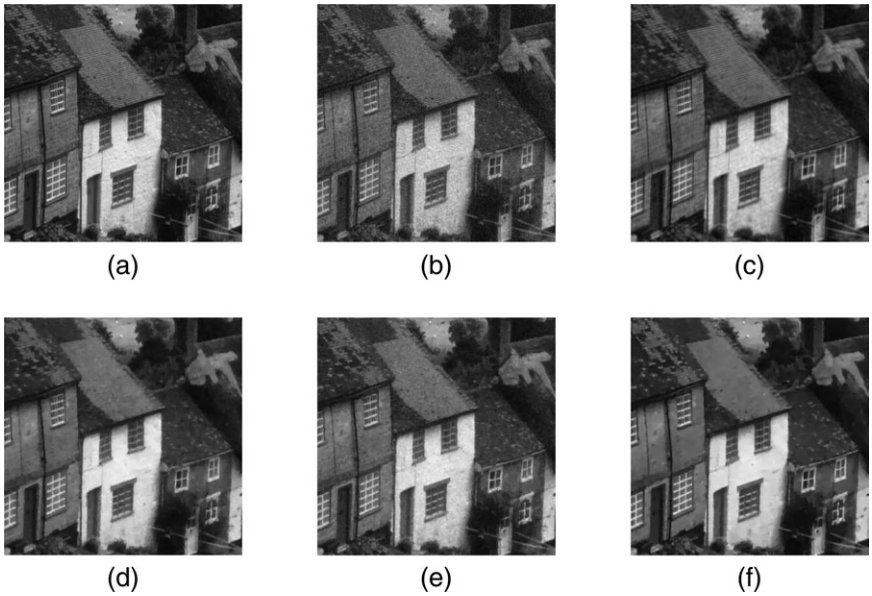

Figure 3. The results by different methods with a Gold Hill image. (a) Original image. (b) Noisy blurred image, $\sigma = 8$ dB. (c) ForCuRD estimate, ISNR = 2.56 dB. (d) FTVd estimate, ISNR = 2.98 dB. (e) TVBregman estimate, ISNR = 3.07 dB. (f) Our method estimate, ISNR = 3.28 dB.

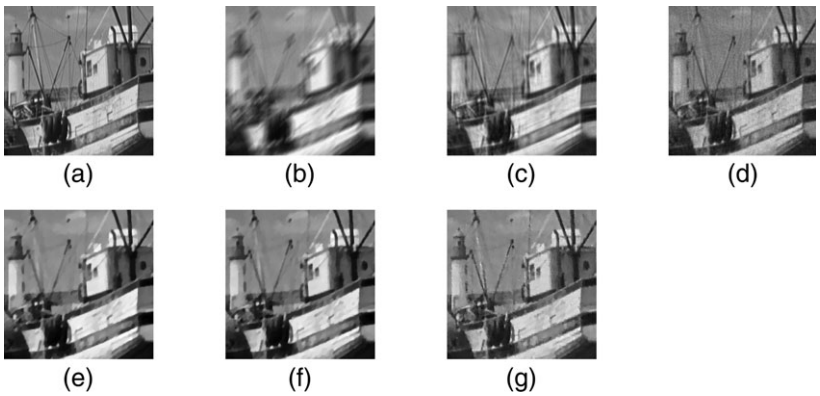

Figure 4. The results by different methods with a boats image. (a) Original image. (b) Noisy blurred image, $\sigma = 2$. (c) ForCuRD estimate, ISNR = 4.53 dB. (d) ForWaRD estimate, ISNR = 4.73 dB. (e) FTVd estimate, ISNR = 4.77 dB. (f) TVBregman estimate, ISNR = 5.16 dB. (g) Our method estimate, ISNR = 5.54 dB.

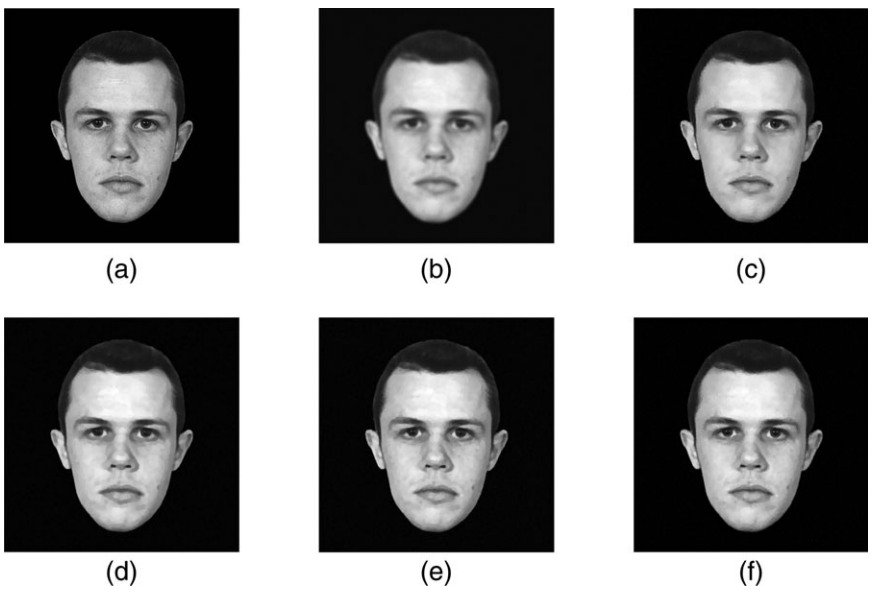

Figure 5. The large format full face images obtained by different methods. (a) Original image. (b) Noisy blurred image. (c) LPA-ICI estimate, ISNR = 5.08 dB. (d) FTVd estimate, ISNR = 4.95 dB. (e) TVBregman estimate, ISNR = 5.28 dB. (f) Our method estimate, ISNR = 5.53 dB.

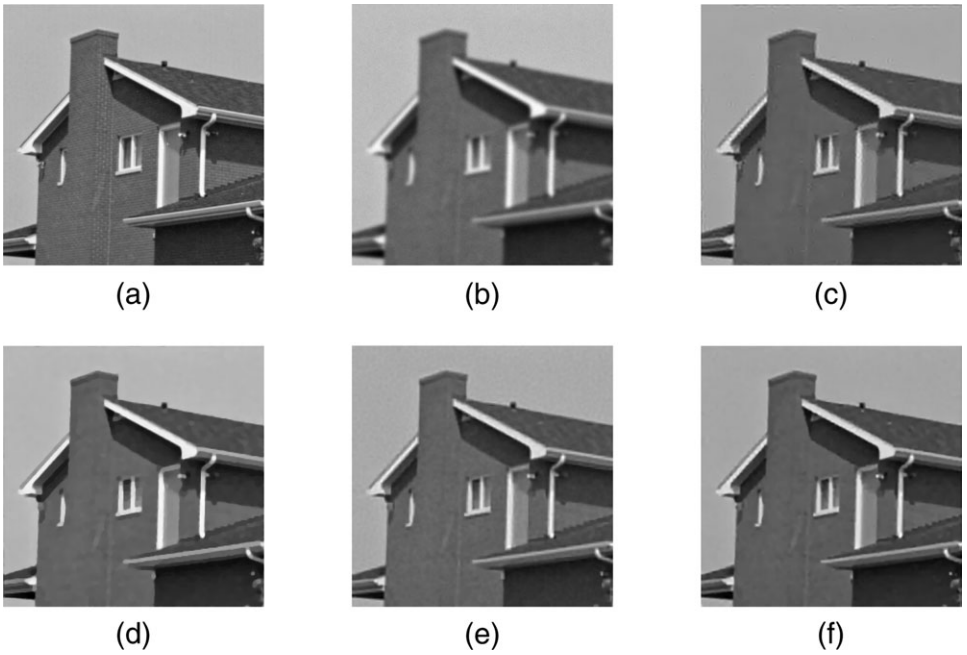

Figure 6. The results of Exp. 8. (a) Original image. (b) Blurred image. (c) ForWaRD result, ISNR = 3.85 dB. (d) FTVd result, ISNR = 4.54 dB. (e) LPA-ICI result, ISNR = 4.64 dB. (f) Our method result, ISNR = 4.96 dB.

variance, σ^2, with a BSNR of 40 dB. We report the simulation results in Table I. Again, our proposed method performs best in the known methods for this problem setup.

In the third experiment, we use the blur filter considered in Patel et al. (2009). The original image of Barbara is blurred by a 5×5 separable filter with weights [1, 4, 6, 4, 1]/16 in both the horizontal and the vertical directions and then contaminated with AWGN with $\sigma = 5$. In this experiment, our method is better than LPA-ICI, ForWaRD, FTVd, and TVBregman.

In the forth experiment, the original image of the 512×512 Gold Hill is blurred by a Gaussian PSF with standard deviation 0.4, the size of PSF is 25×25. The noise variance $\sigma^2 = 64$. We show our result in Table I and the details of the results in Figure 3.

In the fifth experiment, we use the motion blur filter, the length is 11 and the angle is 45°, which corresponds to a 45° motion of 11 pixels. The original image of the 512×512 boats is blurred by this PSF and then contaminated with AWGN with $\sigma = 2$. The details of the images obtained by the different methods

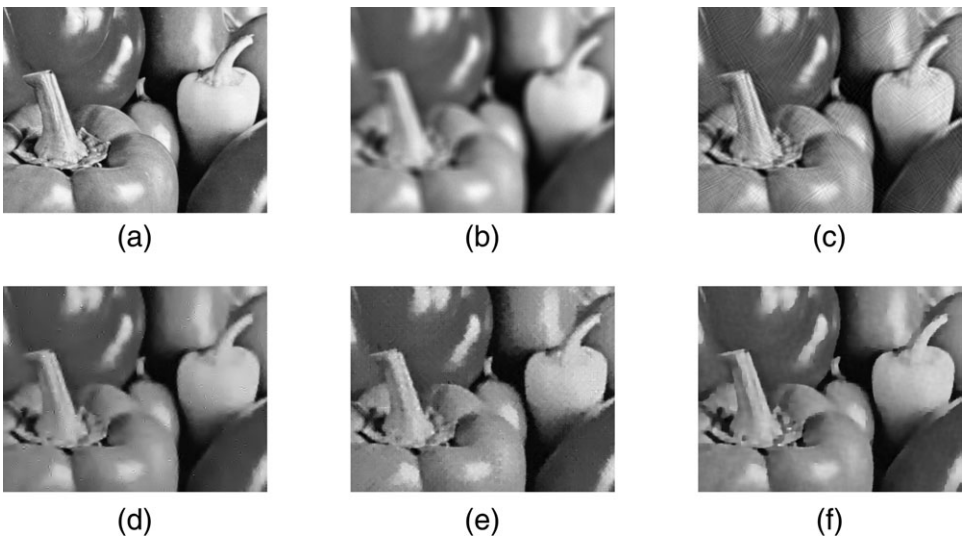

Figure 7. Details of the image deconvolution experiment with a 512×512 Peppers image. (a) Original image. (b) Noisy blurred image, BSNR = 30 dB. (c) ForCuRD estimate, ISNR = 4.53 dB. (d) ForWaRD estimate, ISNR = 3.91 dB. (e) LPA-ICI estimate, ISNR = 4.17 dB. (f) Our method estimate, ISNR = 5.65 dB.

are shown in Figure 4. Again, the proposed algorithm performs the best in terms of ISNR and captures the details better than any of the other methods.

In the sixth experiment, the original image of Boats is blurred by a 19×19 uniform box-car blur, the noise variances $\sigma^2 = 4$. From Table I, we can notice that our method performs the best in terms of ISNR.

In the seventh experiment, we use the 2D $r = 4.5$ circular spot blur filter plus white Gaussian noise with variance $\sigma^2 = 4$. The original image is the 512×512 face image. The large format images obtained by the different methods are shown in Figure 5. The proposed algorithm performs better than the other methods in terms of ISNR and visual quality.

In the eighth experiment, we apply a Gaussian PSF (with standard deviation 1.6) on the House image. The deconvolution results obtained by different methods are reported in Table I. Our method performs yielding ISNR values of 4.96 dB. This experiment shows that our proposed method can provide better reconstruction than some of the competitive deconvolution methods. The details of the images obtained by the different methods are shown in Figure 6.

The performance of the robustness to noise suppression of our method is shown in Figure 7. In this set of tests, the 512×512 Peppers image is blurred by a 9×9 uniform box-car blur and the AWGN is added such that the BSNR = 30 dB. We tested the ForWaRD method (3.91 dB), the LPA-ICI method (4.17 dB), and our proposed method (5.65 dB) using the same Fourier regularization parameter α (not necessarily optimal) for each routine. This set of tests present an important comparison in robustness to noise suppression and an indication of our method's high default tolerance level when the regularization parameter is not chosen optimally.

Additionally, we explain why the partially selected Fourier components would work better briefly. A heuristic justification is provided: our method can be written as $\|\Phi u\|_1 + \frac{\lambda}{2}\| \frac{R}{H} (\frac{|H|^2}{|H|^2+\alpha} Y - HU)\|_2^2$. We find that the image components where $|H(k_1, k_2)| \approx 0$ are not useful for image deconvolution, so $\frac{|H(k_1,k_2)|^2}{|H(k_1,k_2)|^2+\alpha}$ is used to suppress the noise's energy and keep the main energy of image. And different components are given different weights.

IV. CONCLUSION AND FUTURE WORK

In this work, we have proposed a novel image deconvolution method, which is based on image recovery from incomplete measurements in Fourier domain. The motivation of our algorithm is that Fourier shrinkage exploits the Fourier transforms economical representation of the colored noise in herent in deconvolution, and Fourier transform captures maximum colored noise energy using a fixed number of coefficients. When these Fourier coefficients are removed, the energy of the remaining noise is small, while keeping the image's main energy. So, the remaining Fourier coefficients are used to recover the original image under sparse constraints. This is a L1-norm minimization problem. The fundamental principle of compressed sensing shows that the L1-norm optimization problem can recover the image well from the incomplete measurements of it. Furthermore, we use the split Bregman techniques to solve this L1-norm minimization problem.

In this article, we have assumed knowledge of the convolution operator. However, the convolution operator is unknown in many case. In such ''blind'' deconvolution problems, the convolution system must be estimated from observations. It would also be of interest to apply the methods developed here to blind deconvolution.

REFERENCES

L.M. Bregman, The relaxation method of finding the common point of convex sets and its application to the solution of problems in convex programmingm, USSR Comput Math Math Phys 7 (1967), 200–217.

J. Cai, S. Osher, Z. Shen, Linear Bregman iteration for compressed sensing, Math Comput 78 (2009), 1515–1536.

J. Cai, S. Osher, Z. Shen, Split Bregman methods and frame based image restoration, Multiscale Model Simul 8 (2009), 337–369.

E. Candes, J. Romberg, and T. Tao, Stable signal recovery from incomplete and inaccurate measurements, Commun Pure Appl Math 59 (2006), 1207–1223.

K.R. Castleman, Digital image processing, Prentice-Hall, Englewood Cliffs, NJ, 1996.

J.Y. Chang, and J.L. Chen, Classifier-augmented median filters for image restoration, IEEE Trans Instrum Meas 53 (2004), 351–356.

G. Davis, and A. Nosratinia, ''Wavelet-based image coding: An overview'', In Applied and Computational Control Signals, and Circuits, Vol. 1, B.N. Datta (Editor), Birkhauser, Boston, MA, 1999, 112–120.

D.L. Donoho, Nonlinear solution of linear inverse problems by wavelet–vaguelette decomposition, Appl Comput Harmon Anal 2 (1995), 101–126.

M. Elad, B. Matalon, and M. Zibulevsky, Coordinate and subspace optimization methods for linear least squares with non-quadratic regularization, Appl Comput Harmon Anal 23 (2007), 346–367.

M.J. Fadili, and J.-L. Starck, Sparse representations-based image deconvolution by iterative thresholding, 2007 (preprint).

J. Fan, and J.-Y. Koo, Wavelet deconvolution, IEEE Trans Inf Theory 48 (2002), 734–747.

M. Figueiredo, and R.D. Nowak, An EM algorithm for wavelet-based image restoration, IEEE Trans Image Process 12 (2003), 906–916.

T. Goldstein, S. Osher, The split Bregman algorithm for l1 regularized problems, SIAM J Imaging Sci 2 (2009), 323–343.

A.D. Hillery, and R.T. Chin, Iterative Wiener filters for image restoration, IEEE Trans Signal Process 39 (1991), 1892–1899.

A.K. Jain, Fundamental of digital image processing, Prentice-Hall, Englewood Cliffs, NJ, 1989.

I.M. Johnstone, G. Kerkyacharian, D. Picard, and M. Raimondo, Wavelet deconvolution in a periodic setting, J R Stat Soc B: Stat Methodol 66 (2004), 547–573.

J. Kalifa, S. Mallat, and B. Rouge, Deconvolution by thresholding in mirror wavelet bases, IEEE Trans Image Process 12 (2003), 446–457.

V. Katkovnik, K. Egiazarian, and J. Astola, A spatially adaptive nonparametric regression image deblurring, IEEE Trans Image Proces 14 (2005), 1469–1478.

L. Landweber, An iterative formula for Fredholm integral equations of the first kind, Am J Math 73 (1951), 615–624.

L.B. Lucy, An iterative technique for the rectification of observed distributions, Astron J 79 (1974), 745–754.

J.W. Ma, Improved iterative curvelet thresholding for compressed sensing and measurement, IEEE Trans Instrum Meas 60 (2011), 126–136.

R. Neelamani, H. Choi, and R.G. Baraniuk, ForWaRD: Fourierwavelet regularized deconvolution for ill-conditioned systems, IEEE Trans Image Process 52 (2004), 418–433.

R.N. Neelamani, M. Deffenbaugh, and R.G. Baraniuk, Texas two-step: A framework for optimal multiinput single-output deconvolution, IEEE Trans Image Process 16 (2007), 2752–2765.

S. Osher, M. Burger, D. Goldfarb, J. Xu, and W. Yin, An iterative regularization method for total variation-based image restoration, Multiscale Model Simul 4 (2005), 460–489.

M. Patel, G.R. Easley, and D.M. Healy Jr., Shearlet-based deconvolution, IEEE Trans Image Process 18 (2009), 2673–2685.

W.H. Richardson, Bayesian-based iterative method of image restoration, J Opt Soc Amer 62 (1972), 55–59.

J. Starck, M.K. Nguyen, and F. Murtagh, Wavelets and curvelets for image deconvolution: A combined approach, Signal Process 83 (2003), 2279–2283.

H. Takeda, S. Farsiu, and P. Milanfar, Deblurring using regularized locally adaptive kernel regression, IEEE Trans Image Process 17 (2008), 550–563.

C. Vonesch, and M. Unser, A fast thresholded Landweber algorithm for wavelet-regularized multidimensional deconvolution, IEEE Trans Image Process 17 (2008), 539–549.

Y. Wang, J. Yang, W. Yin, and Y. Zhang, A new alternating minimization algorithm for total variation image reconstruction, SIAM J Imaging Sci 1 (2008), 248–272.

W. Yin, S. Osher, D. Goldfarb, and J. Darbon, Bregman iterative algorithms for l1-minimization with applications to compressed sensing, SIAM J Imaging Sci 1 (2008), 142–168.